

We are IntechOpen, the world's leading publisher of Open Access books Built by scientists, for scientists

6,900

Open access books available

186,000

International authors and editors

200M

Downloads

Our authors are among the

154

Countries delivered to

TOP 1%

most cited scientists

12.2%

Contributors from top 500 universities



WEB OF SCIENCE™

Selection of our books indexed in the Book Citation Index
in Web of Science™ Core Collection (BKCI)

Interested in publishing with us?
Contact book.department@intechopen.com

Numbers displayed above are based on latest data collected.
For more information visit www.intechopen.com



Microfluidic Multiple Chamber Chip Reactor Filled with Enzyme-Coated Magnetic Nanoparticles

Ferenc Ender, Diána Weiser and László Poppe

Additional information is available at the end of the chapter

<http://dx.doi.org/10.5772/62512>

Abstract

In this chapter, a novel microfluidic device (MagneChip) is described which comprises microliter volume reaction chambers filled with magnetically fixed enzyme-coated magnetic nanoparticles (*ec*MNPs) and with an in-line UV detector. In the experiments, MNPs with phenylalanine ammonia-lyase (PAL)—an enzyme which catalyzes the deamination of L-phenylalanine (Phe) to (E)-cinnamate in many organisms—immobilized on the surface were applied as biocatalyst to study the characteristics of the MagneChip device. In the reaction chambers of this microfluidic device, the accurate in situ quantization of the entrapped MNPs was possible using a resonant coil magnetometer integrated below the chambers. Computational fluid dynamics (CFD) calculations were used to simulate the flow field in the chambers. The enzyme-catalyzed biotransformations could be performed in the chip with excellent reproducibility and of repeatability. The platform enabled fully automatic multiparameter measurements with a single biocatalyst loading of about 1 mg PAL-*ec*MNP in the chip. A study on the effect of particle size and arrangement on the catalytic activity revealed that the mass of *ec*MNPs fixed in the chamber is independent of the particle diameter. Decreasing the particle size resulted in increasing catalytic activity due to the increased area to volume ratio. A binary mixture of particles with two different particle sizes could increase the entrapped particle mass and further the catalytic activity compared to the best uniform packing. The platform enabled a study of biotransformation of L-phenylalanine and five unnatural substrates by consecutive reactions using same PAL-*ec*MNP loading. With the aid of the platform, we first demonstrated that PAL can catalyze the ammonia elimination from the noncyclic propargylglycine as substrate.

Keywords: Magnetic nanoparticles, Magnetic chip reactor, Microfluidic reactor, Enzyme reaction, Phenylalanine ammonia-lyase

1. Introduction

Microreactors are usually defined as miniaturized reaction systems fabricated using methods of microtechnology and precision engineering. The term “microreactor” is the proposed name for a wide range of devices, having typically submillimeter channel dimensions which can be further divided into submicron sized components, for example, microparticle and nanoparticle carriers [1].

Before evolution of microreactor technology, the traditional way to conduct solution phase synthesis and analysis was the batch mode in stationary reactors with stirring or shaking to mix the reactants. Nowadays, microstructured devices offer greatly enhanced performance compared with conventional batch systems due to effects arising from the microscale domain:

- Batch processes are space-resolved; therefore, the process must be readjusted in each demand for larger product quantities. In contrast, flow microreactor processes are time-resolved; therefore, the output of the reaction is determined by the flow rate and the operation time, and no further optimization is needed. This also leads to accelerated process development and enhanced safety due to smaller reactor volumes [2].
- Microreactors with high surface-to-volume ratio (SVR) are able to absorb the heat evolving in an exothermic reaction more efficiently than any batch reactor. Therefore, the temperature distribution inside the microreactor is homogenous in the whole volume. In contrast, small SVR usually leads to uneven temperature distribution in large-scale batch reactors, decreasing the product yield [2].
- Mixing quality is crucial for many reactions, where the molar ratio between the reactants needs to be controlled precisely. Short diffusion paths provide efficient mixing in microreactors, which overrides the achievable mixing efficiency of batch reactors [2].
- In biocatalytic applications, the efficiency of the microreactor can be further improved by immobilization of enzymes on nanoscale carriers accommodating in the reactor. Reusability of the biocatalyst makes the process economical and more environmentally friendly.
- To perform similar analyses in shorter timescale even in parallel is an anticipated objective for screening and routine use in protein and enzyme research [3]. A desirable goal is the high throughput screening of enzymes and their substrates and inhibitors. The prospective fields of application of microreactors are quite wide and include biotechnology, as well as combinatorial chemistry and enzyme-targeted drug discovery [4].
- Analytical systems which comprise microreactors are characterized by outstanding repeatability and reproducibility, due to replacing iterative steps in batch and discrete sample treatment by flow injection systems [4]. Benefitting from system automation, this also eliminates errors associated with manual protocols.
- Small reagent volume is also a benefit of microreactors enabling economical and efficient screening of novel reaction paths and substrates.

- Microreactors have a high potential in industry, as developments by microreactors can be faster transferred into production at lower costs than batch processes.

Despite of the rapid development of enzymatic microreactors in the recent decade, important design questions still need to be answered.

Reaction kinetics is a key parameter of device design. Widely used kinetic parameters are deduced from the Michaelis–Menten model, which is valid only in batch reactions. In flow systems, the flow effects should be also considered. Immobilization of the enzymes causes further complication in modeling. Immobilization may affect the intrinsic kinetic parameters and may influence the availability of the enzyme. The kinetic model should also consider that the liquid phase containing the substrate and product is moving compared to the solid phase containing the immobilized enzyme.

When supported catalyst-filled microreactors are used, reproducible filling of the supported catalyst into the reactor space is not always straightforward. Even more challenging is the quantification of the actual load of the carriers.

Long-term stability of the reactor and the reproducibility of the measurements may be affected –among other factors– by the flow rate, the substrate concentration, and the morphology of the immobilized biocatalyst.

This chapter presents results carried out by a microfluidic microreactor system, the so called MagneChip platform including four serial reaction chambers with individually removable permanent magnets. The results were achieved by experiments using phenylalanine ammonia-lyase (PAL) from *Petroselinum crispum* immobilized on the surface of magnetic nanoparticles (MNPs) and filled into one or more chamber of the MagneChip.

Biotransformations with PAL under different conditions were performed mostly using the natural substrate L-phenylalanine to study

- the reproducibility of biotransformation in the microreactor system,
- the effects of the long-term use and cyclic reuse of the biocatalyst on the biocatalytic activity,
- the effects of the particle size on the biocatalytic activity,
- the optimal substrate concentration and flow rate of the in-chip biotransformation,
- the effect of immobilization and the use of flow microreactor on the kinetic constants, and
- the biotransformations of further substrates with PAL.

2. Background

2.1. Microreactors

Analytical systems which comprise microreactors are characterized by outstanding repeatability and reproducibility, due to replacing batch iterative steps and discrete sample treat-

ment by flow injection systems [4]. The possibility of performing similar analyses in parallel is an attractive feature for screening and routine use [3]. Microreactors have been integrated into automated analytical systems, as well as providing benefits from system automation, and this also eliminates errors associated with manual protocols [4].

Applications of microreactors can be divided into three classes [4]:

- Organic synthesis, when a target molecule is formed from components in flow
- Analytical use of biocatalysts to transform an analyte difficult to measure to an easy to measure form
- Screening of substrates and enzymes examines their kinetic characteristics

Microreactor systems can be further divided into classes based on the physical localization of the catalyst:

Laminar flow reactors: The majority of the commercial flow synthesis systems utilize laminar flow with soluble components and enzymes [5]. Losing the catalyst is a major drawback of this technique.

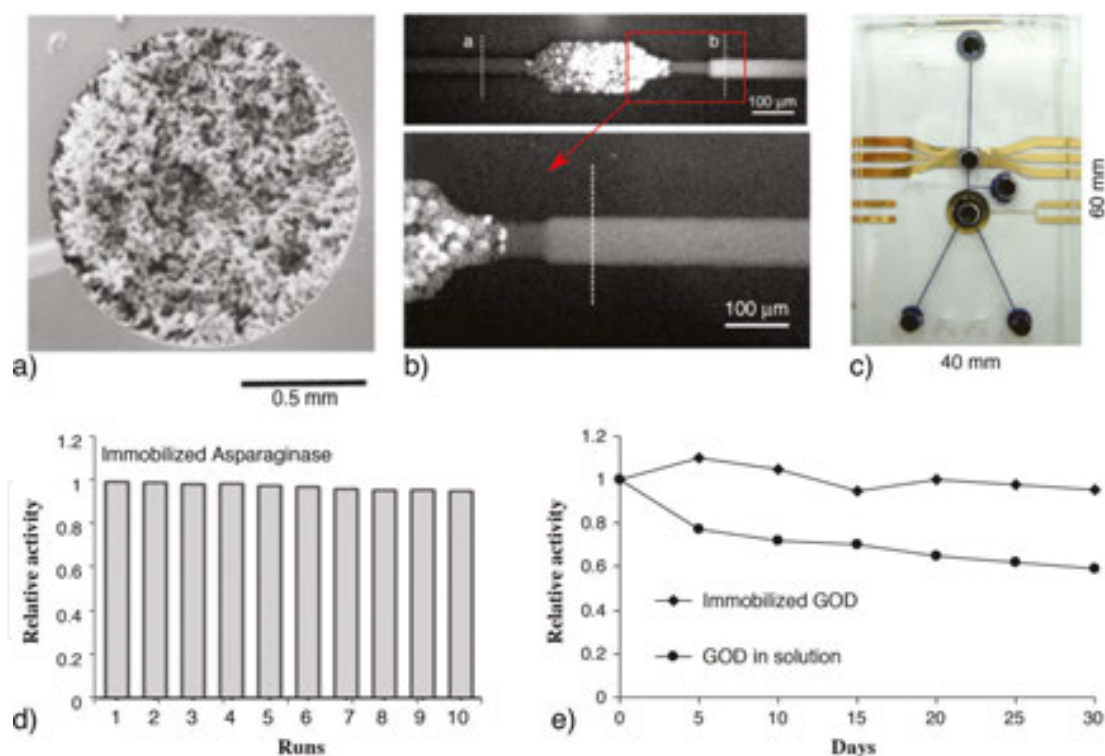


Figure 1. Lab-on-a-chip microreactors: (a) a monolith silica reactor [8], (b) a packed bed silica reactor [9], and (c) a packed bed MNP reactor [10]. Stability of immobilized enzymes: (d) after reuse of asparaginase in 10 cycles, 10 min each [7] and (e) during long-term operation of immobilized GOD [8].

Filled reactors: Microreactors utilizing immobilized catalysts (e.g., enzymes) have many advantages over the traditional flow reactors. First of all, the catalyst (enzyme) can be recycled after usage; therefore, the process is more economical and environmental friendly. The

reactions are highly reproducible as the catalyst (enzyme) concentration is fixed in the system. Immobilization of enzymes often causes decrement in biocatalytic activity and choosing the appropriate immobilization technique is challenging [6]. It was reported that immobilized asparaginase retained 95.7% of its activity after 10 cycles of use [7] (**Figure 1d**), while immobilized glucose oxidase enzyme (GOD) retained 97% of its original activity after cyclic regeneration and reuse [8]. Immobilization often extends the long-term stability and temperature resistance of the enzymes, and in several cases, even the catalytic activity is increased compared with the soluble form. Immobilized asparaginase retained the 72.6% of its original activity for 10 weeks [7], and immobilized GOD retained the 95% of its activity [8] (**Figure 1e**) for 30 days.

The reactors filled with immobilized (bio)catalyst can be further divided into two groups according to the type of the supporting material of the (bio)catalyst:

- *Monolith reactors*: The reactor is defined as monolith reactor where the supporting material is fixed in the reactor volume, and the (bio)catalyst is nonremovable; therefore, the chip is single use. Nanostructured materials are used to further increase the SVR. Examples include silica monolith reactors [8] (**Figure 1a**) or most recently reactors incorporating nanofibrous material made by electrospinning [11].
- *Packed bed reactors*: The reactor is defined as packed bed reactor where the supporting materials are beads, even on microscale or nanoscale. The (bio)catalyst is immobilized onto their surfaces. Nanotechnology enables functional modifications of the beads, for example, making them magnetic. The reactor can be loaded with the suspension of the beads (**Figure 1b**) and viscous [9] or magnetic [12, 13] forces are utilized to keep the particles fixed in the reaction chamber.

Kinetic studies could be carried out with ease in microreactors by changing the attributes of the reaction, for example, the inflow substrate concentration. Because the most often used Michaelis–Menten model cannot be applied to flow reactors; in several cases [9, 14], the Lilly–Hornby model [15] was applied. Dependency of the kinetic parameters on the flow rate—and occasionally on further other parameters—was reported in many cases implying the limitations of the Michaelis–Menten model [8, 9, 14, 16].

In every on-chip study, K_m and k_{cat} as kinetic parameters were determined using various ways of product quantification such as capillary electrophoresis (CE) [7], amperometry [8], and fluorescent imaging [9, 16].

References	Enzyme	Method	Reusability	Stability	Particle	[E] measurement
Mu et al. [7]	Asparaginase	Michaelis–Menten, LB plot	10 cycles 100 min	10 weeks	MNP	Out of chip
		K_m, V_{max} CE out of chip	95.70%	72.60%	12 nm	Supernatant

References	Enzyme	Method	Reusability	Stability	Particle	[E] measurement
He et al. [8]	GOD	Michaelis–Menten, EH plot K_m, k_{cat} Amperometry, on-chip	97%	30 days 95%	Monolith reactor silica	Out of chip Absorbance
Kerby et al. [14]	Alkaline phosphatase	Lilly–Hornby K_m, k_{cat} Fluorescent imaging	N/A	N/A	Silica Microbeads	In chip Optical
Slovakova et al. [16]	Trypsin	Michaelis–Menten, LB plot K_m, k_{cat}	80%	N/A	MNP 600 nm	Approximated
Seong et al. [9]		Lilly–Hornby K_m Fluorescent imaging	N/A	N/A	Microbeads 15 μ m	Optical

Table 1. Lab-on-a-chip microreactors with immobilized enzymes.

2.2. Magnetic nanoparticles in microreactors

The importance of MNPs as potential carriers of biomolecules is growing rapidly in biotechnology and biomedicine. In LoC systems, nanosized magnetic particles provide quasi-homogeneous systems, high dispersion, high reactivity, low diffusion limits, and possibility of magnetic separation. The MNPs are usually collected in microsized reaction chambers. The collection and separation from the fluid stream are accomplished by external magnetic field. Such microreactors were found to be highly effective in biodetection [24], biocatalytic [17], and bioanalytical [18] applications (**Table 1**).

Magnetite nanoparticles exhibit superparamagnetic or soft ferromagnetic behavior with high saturation magnetization resulting in high permeability values [19]. To date, magnetic manipulation of magnetic beads utilizing a magnetic bead separator array seems to be one of the most promising technique of precise handling of biocatalysts in chip. Do et al. [12] developed a microfluidic platform, where the magnetic field was concentrated between permalloy patterns (50×100) to produce a high magnetic field gradient over the edges of them, thus being able to trap the magnetic beads. Li et al. [13] used external hard magnet to develop a concentrated magnetic field perpendicular to the channel at a certain position of the chip. The particles accumulated at the designated place. Slovakova et al. [16] used a pair of hard neodymium magnets positioned in a given angle to develop a magnetic field parallel to the channel structure. It was reported that in this case, the particles are arranged parallel with the

channel axis, and also, the reaction efficiency was reasonably higher than in orthogonal configurations. Lien et al. [10] used an integrated electromagnet with active cooling for the entrapment of the magnetic particles in the reaction chamber (**Figure 1c**).

Because of the widespread applications of MNPs in biotechnology, biomedical, and material science, more and more synthesis techniques have been developed to obtain different kinds of MNPs. Exhaustive discussions on the available synthesis techniques (e.g., coprecipitation, microemulsion, thermal decomposition, solvothermal, sonochemical, microwave assisted, chemical vapor deposition, combustion synthesis) can be found in several reviews [20, 21]. The synthetic methods will determine the shape, the size distribution, size, the surface chemistry of the particles, and consequently their magnetic properties. Various optimization methods could be used to obtain proper MNPs suitable for the desired research and commercial applications [21].

In our study, the surface of MNPs was chemically modified by sol-gel method, which resulted in the formation of a core-shell silica-MNP carrier. Then, the surface was functionalized by epoxy groups, which were able to form stable, covalent binding with the amino, thiol, or hydroxide groups of the enzyme. The immobilization of *PcPAL* was carried out in liquid phase. For a detailed description, see [18]. After immobilization, negligible protein contents in the supernatants of the washing procedure were determined by the Bradford assay method [22]. The resulted enzyme-coated magnetic nanoparticles (*ecMNPs*) were used in two size variations, with 250 and 600 nm diameters. Where otherwise not indicated the nominal *ecMNP* diameter is 250 nm.

3. The MagneChip platform: construction and operation

MagneChip is a microfluidic platform centered on a chip consisting of several reaction chambers enabling accumulation (and release) of MNPs. This magnetic microreactor chip can utilize the benefit of excellent separation ability of MNPs in magnetic field. In various applications, the MNPs covered by biologically active molecules (e.g., bioreceptors) are immobilized on their surfaces may be used. Magnetic techniques enable anchoring the particles inside certain compartment of microreactors, where the accumulated magnetic particles can form a dense layer. After filling (in a consecutive step), reagents can flow through the chip, while bioreaction occurs inside the microchambers and the resulted product flows through the chip. The outflow can be collected and/or quantified outside the chip, for instance by absorbance method. Because the enzyme to be immobilized on the MNP surfaces can be chosen freely, a wide variety of applications are possible (**Figure 2**). Taking the advantage of the continuous-flow operation, product formation can be monitored for a long time under various conditions over the same anchored *ecMNP* layer. MagneChip can be reinitialized periodically which enables multiparameter experiments, and therefore, reaction kinetics can be characterized in a fully automated way. Because the flow control system of the platform allows changing the actual substrate over the *ecMNP* layer, reactions can be screened even with unexplored substrates (**Scheme 1**). This feature renders MagneChip as a tool for substrate discovery as well.

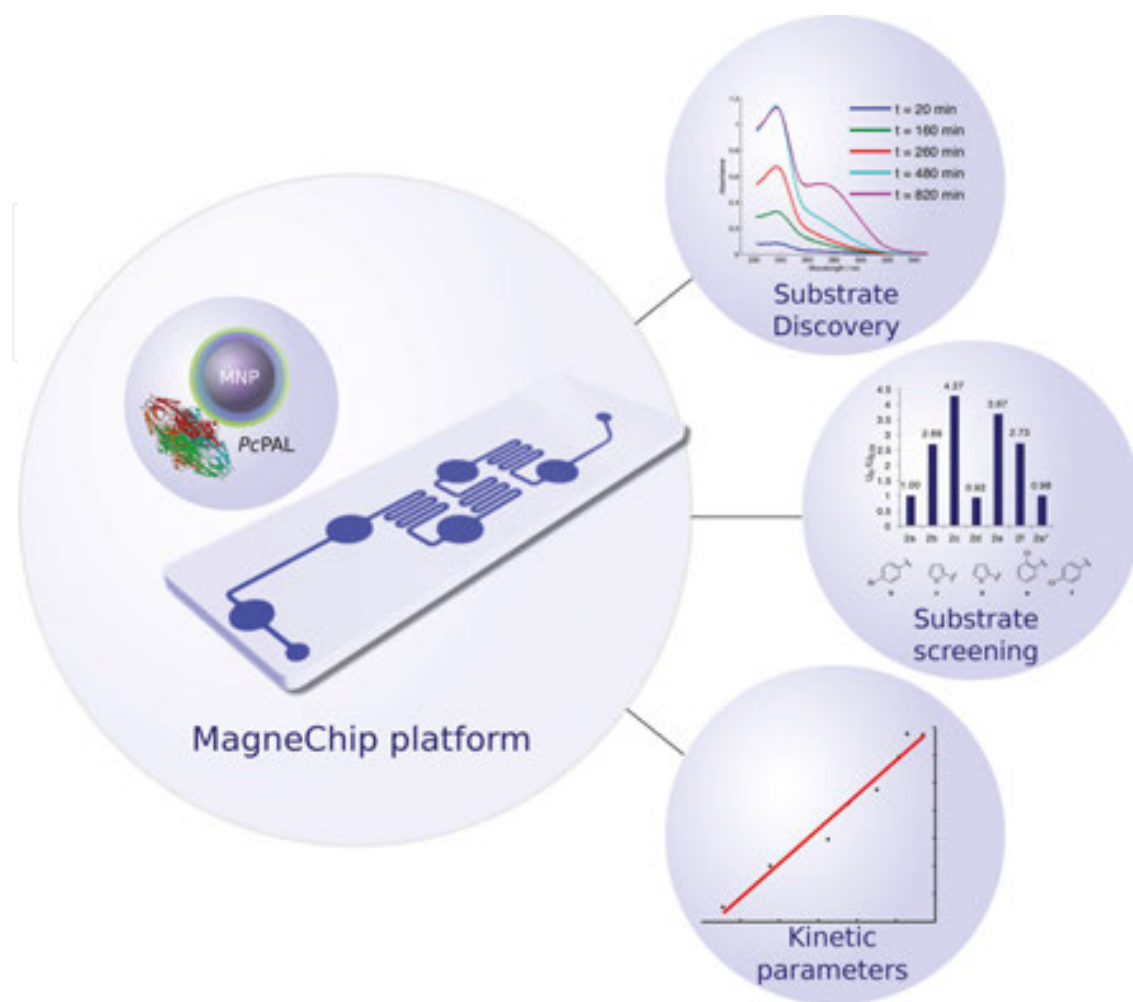
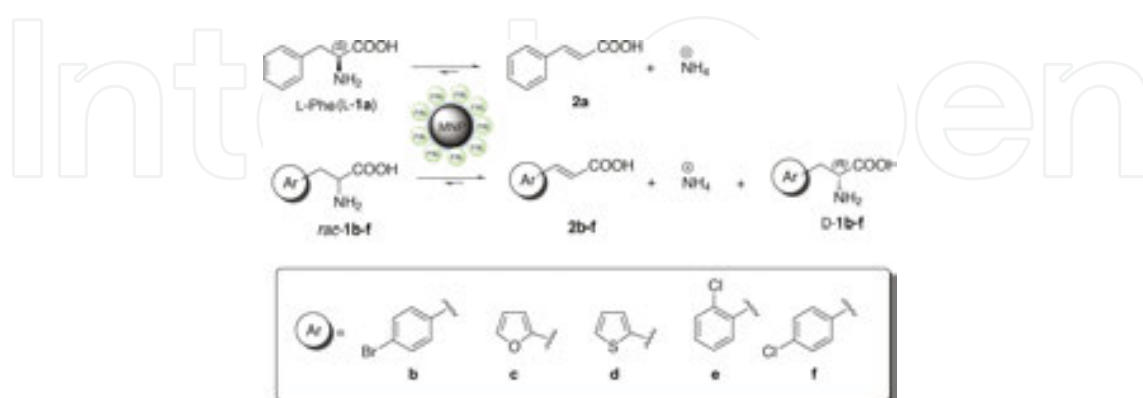


Figure 2. Possible applications of MagneChip platform. Reaction chambers are filled with bio-functionalized magnetic nanoparticles, product formation is measured by in-line UV detector.



Scheme 1. Ammonia elimination from different amino acids (**1a-f**) catalyzed by *PcPAL* immobilized onto MNPs within the MagneChip.

3.1. Basic aims and principles

A microfluidic test bench was developed for carrying out microreactor experiments with MagneChip (Figure 3). The test bench consisted of two syringe pumps for dispensing reagents, a thermostable chip holder and a zoom microscope for the optical inspection of the chip. The chip holder had four magnet drawers enabling to push permanent magnets under reaction chambers of the chip and also pull them out as the magnetic field is no longer required.

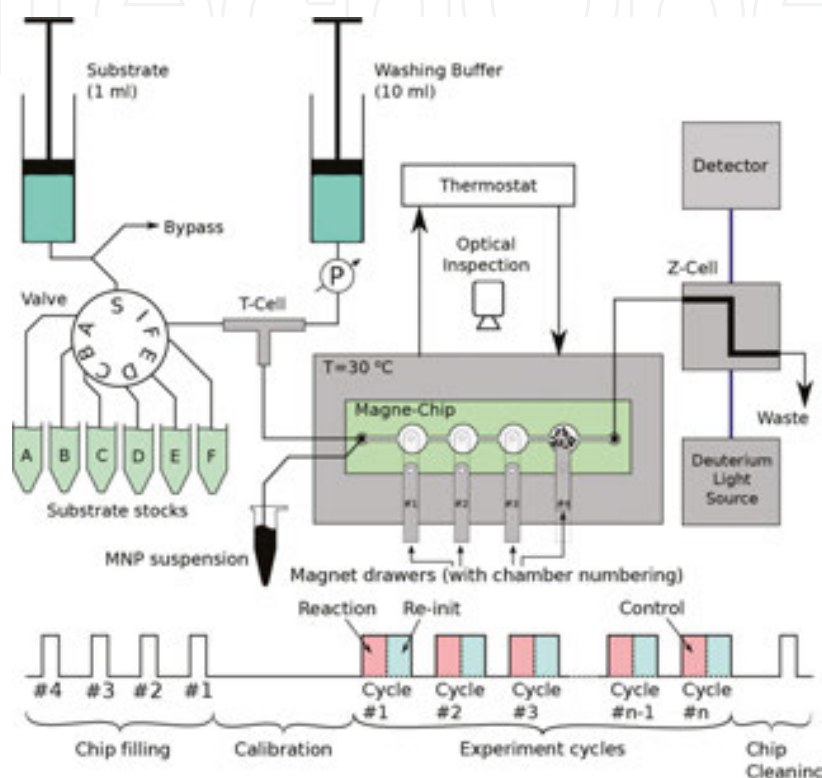


Figure 3. Schematic diagram of the fluid control system of MagneChip platform [22].

MagneChip reaction chambers (volume of $\sim 1 \mu\text{l}$) were designed to accomplish the following requirements:

- Because (bio)chemical reaction occurred inside the reaction chambers operating under continuous-flow conditions, a relative homogenous flow velocity distribution was required. This condition could be fulfilled because laminar flow was developed in the chamber.
- MNPs were accumulated in the chambers, and their drifting was prevented by an external magnetic field. The critical flow rate and the amount of accumulated *ec*MNPs could be increased using prolated channels providing sufficient amount of (bio)catalysts to reach reasonable conversion of the desired reaction.
- A resonant coil magnetometer was installed under the reaction chambers. Using the magnetometer, the accumulated amount of *ec*MNPs could be measured with high accuracy.

A four reaction chamber MagneChip layout is presented in **Figure 4a**. CFD simulations revealed that the flow velocity distribution inside of the chambers varied in a scale of two (**Figure 4b**). Depending on the typical flow rates used in MagneChip, reaction residence time in the chambers may vary from 1 to 10 s (**Figure 4c**).

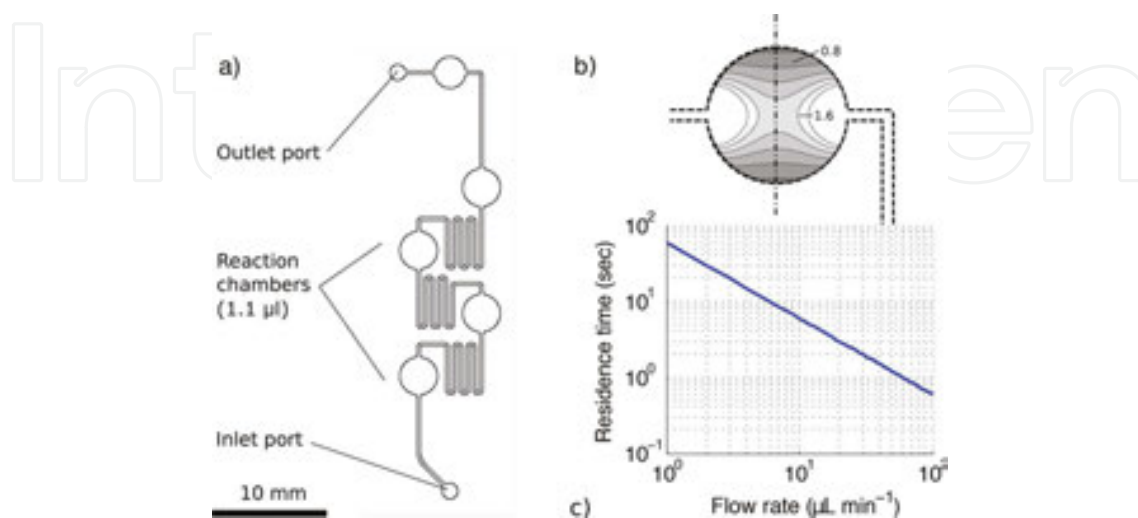


Figure 4. (a) Layout of the four chamber MagneChip; (b) flow velocity distribution inside the reaction chambers (units are in mm s^{-1}); (c) residence time vs. flow rate in MagneChip reaction chambers.

3.2. Construction method of MagneChip

Figure 4a depicts the arrangement of a four-chamber chip used for testing the enzymatic reactions.

The chip was constructed by PDMS molding technology. SU-8 photoresist structures were prepared as a molding master, resulting in a channel height of $110 \mu\text{m}$. PDMS was poured on the master and was kept on room temperature for 1 day. After cross-linking, the PDMS replica was released and the PDMS channel bodies were bonded to standard microscope glasses after oxygen plasma treatment. Some of the chips were equipped with a resonant coil magnetometer placed under the chambers for MNP quantity measurement [23]. The coil was embedded in an intermediate PDMS layer. For further construction details, see [23].

3.3. Method of MNP quantification in the reaction chambers

The magnetic behavior of MNPs initiated the development of an inductive method to quantify the nanoparticles. The measurement is based on the resonance frequency shift of a passive electrical resonant circuit, where a flat inductor coil integrated in a silicone elastomer film acts as a sensor. From the suspension of MNPs flowing into the chip, MNPs were anchored within the reaction chambers by external permanent magnets. The *ec*MNP amount inside the chamber affected the inductance; therefore, the resonance frequency was changed. The method also enabled on-line monitoring of the actual *ec*MNP quantity in the chamber. This test arrange-

ment enabled to study the effect of particle size and arrangement on the chamber filling MNP mass and also on the catalytic activity of the PAL bound to the *ec*MNPs [23].

3.4. Operation methods of MagneChip

3.4.1. Fluid handling steps

The experiments in MagneChip (**Figure 3**) involved four steps: (1) filling up the chip with MNPs, (2) absorbance calibration, (3) experiment cycles, and (4) chip cleaning.

Chip filling. In the chip-filling step, an MNP suspension was driven through the chip by applying a slight air pressure (0.2–0.3 bar) to the vial containing the MNP suspension and connected to the inlet of MagneChip via a PTFE tube (**Figure 3**) at 25°C. During the filling process, the MNPs were accumulated in the reaction chambers due to the permanent magnets placed in moveable drawers enabling “on/off” switching of the magnetic field. Once the chamber most distant from the inlet (**Figure 3, Chamber 4**) was saturated, the permanent magnet of the chamber at preceding position was turned on (**Figure 3, Chamber 3**). The same procedure was repeated (**Figure 3: Chambers 2 and 1**) until all chambers were filled up. Each chamber of the MagneChip device could capture ca. 250 µg of *ec*MNP biocatalyst [23].

Calibration and experiment cycles: During the forthcoming steps, the valve at the inlet of the MagneChip (**Figure 3**) was switched to the substrate (reagent) circuit. The flow controller performed the dosage of the substrate and other chemicals as dictated by the programmed sequence.

Chip cleaning: At the final, chip-cleaning step, the magnetic drawers of the MagneChip (**Figure 3**) were drawn out and a washing solution was driven through the chip to remove *ec*MNPs.

The individual steps in a series of experiments, called experiment cycle (**Figure 3, Experiment cycles**), involved a *Reaction step* and a *Re-initialization step*. A series of experiments could consist of several experiment cycles depending on the number of parameters to be changed.

Reaction step. In a *Reaction step*, a substrate-containing solution was flowing through the chip at a constant flow rate, and the specific absorbance of the product was continuously monitored in the outflow of the chip.

Re-initialization step. In the *Re-initialization step*, the feed of the substrate-containing solution was stopped, and the chip was flushed with a washing buffer, while the magnetic particles were retained by the permanent magnets.

3.4.2. Reaction step variants

The substrate feed (with continuous monitoring of the absorbance in the outflow at a previously selected wavelength) was accomplished according to one of the following variants. The cycle ended when the predesigned step time had been passed or when the reaction reached saturation.

- *Repeatability test.* The feed of the substrate started (1st cycle) or continued at unchanged flow rate.
- *Flow rate test.* The feed of the substrate started (1st cycle) or continued, while the flow rate changed cycle by cycle.
- *Substrate concentration test.* The substrate-containing solution and the washing buffer were feed in parallel at a predesigned ratio resulted in a predefined dilution of the substrate at the chip inlet. The dilution ratio could be different cycle by cycle.
- *Substrate screening.* The actual substrate was loaded into the substrate syringe through a bypass valve from the actual container of the substrate stock (A-F, in **Figure 3**), and the feed of the substrate began at a predefined flow rate. To change to the next substrate, a *Re-initialization step* was performed, followed by loading the next substrate into the substrate syringe from the substrate stock (A-F).

3.5. Quality assessment of the operations in MagneChip

A series of subsequent measurements performed by the system were considered as reliable if all the following conditions were met [22]:

- independent measurements were reproducible using the same type of *ecMNP* biocatalyst,
- the product of the enzyme reaction could be measured selectively in the UV–Vis range,
- product and substrate could be completely removed through the washing steps,
- the enzymatic activity of the *ecMNP* biocatalyst remained unchanged during the measurement
- and last but not least, the *ecMNP* layer in the magnetic reactors remained unharmed during the measurement cycles.

In order to test the fulfillment of the first group of conditions, a control measurement was performed after each series of experiments; that is, the first step of the sequence was repeated in the last step under the same conditions, and the specific activity of the immobilized biocatalyst (U_B) at saturation concentrations of L-phenylalanine (L-**1a** in **Scheme 1**) in the first and last cycles was compared.

3.5.1. Reproducibility of the individual measurements

Reproducibility of the chip-filling process: The first single chamber of the MagneChip was filled with MNP suspension. Biotransformation of L-**1a** to **2a** (**Scheme 1**) was performed in flow-through mode and monitored by in-line UV–Vis. After reaching the stationary state (i.e., constant level of product formation), the magnet of the chamber was released and the *ecMNPs* were captured in the next chamber. The experiments performed in three consecutive chambers were repeated three times resulting in $U_B = 8.01 \pm 0.14 \mu\text{mol g}^{-1} \text{min}^{-1}$ [22].

The filling–refilling results indicated that neither that the homogeneity of the MNP suspension nor the filling procedure of the chambers had remarkable effect on the reproducibility of

the measurements. The significant difference between the U_B values of MNP biocatalyst in shake vials and in MagneChip indicated increased effectivity of the biocatalysts in MagneChip device [22].

Reproducibility of independent measurements: Biotransformation of L-phenylalanine (**L-1a**) to (E)-cinnamic acid (**2a**) by MNP biocatalyst suspension (**Scheme 1**) was performed in shake vial as three parallel reactions and resulted in $U_B = 2.91 \pm 0.08 \mu\text{mol g}^{-1} \text{min}^{-1}$ ensuring that the homogeneity of the MNP suspension was sufficient [22].

3.5.2. Optical inspection of the reaction chambers

During the experiments, the chip was optically inspected by a zooming microscope and a monochrome hi-speed smart camera. Before evaluating the measurement sequence, the plan view of the chip was stored as a reference (Π_{ref}). At the end of the step i of the measurement sequence, the plan view of the chip was sampled again ($\Pi_{\text{seq},i}$) and it was compared to the reference as follows [22]:

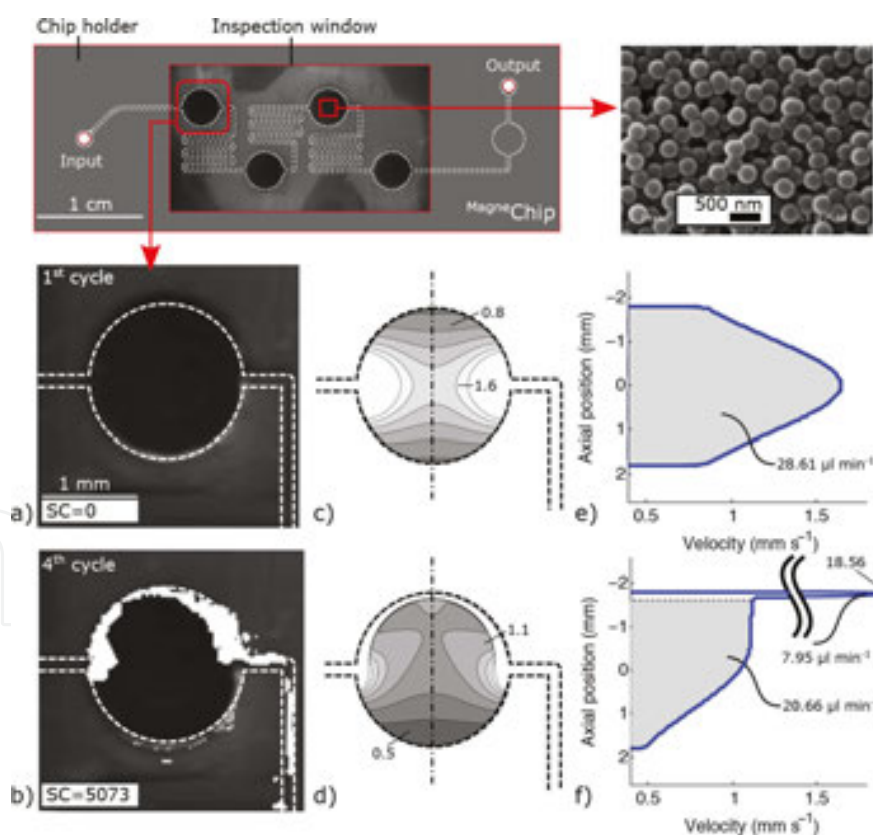


Figure 5. MagneChip device with four MNP-filled and external magnet-equipped microchambers (top left) and SEM image of the MNP layer (top right). The effect of air bubble passage through the reaction chamber [(a)–(f)]: (a) photograph, before passage; (b) difference image (difference score $SC = 5073$), after passage; (c) calculated flow velocity field before and (d) after the passage; (e) velocity profile in the middle cross section of the chamber before and (f) after the passage [22].

$$\Pi_{diff}(j,k) = \begin{cases} \Pi_{ref}(j,k), & \Pi_{ref}(j,k) - \Pi_{seq,i}(j,k) < 0 \\ 0, & \Pi_{ref}(j,k) - \Pi_{seq,i}(j,k) \geq 0 \end{cases}$$

where (j,k) are the pixel coordinates of the plan view image; therefore, the changes in accordance to the reference image are indicated by white pixels. The total number of white pixels is defined as *chamber difference score* (SC) used as a marker for describing the changes of the MNP layer arrangement. Therefore, the changes compared with the image of the first cycle (reference) were indicated by white areas during the consecutive cycles of the measurement.

In practice, SC values under 2000 reflected to negligible changes. However, $SC > 3000$ indicated serious structural change of the *ecMNP* layer, for instance, the complete breakthrough of a bubble (**Figure 5b**) [22]. Air bubbles usually did not split at the channel entrance, rather passed at one side along the chamber wall. Numerical simulations revealed (**Figure 5c–f**) that the velocity profile became asymmetric due to the bubble passage and the overall mass flow rate through the porous MNP layer significantly decreased ($28.6\text{--}20.7 \mu\text{L min}^{-1}$, roughly 72% of its original value), while the remaining fluid passed through the developed tunnel. The passing bubble could drift away particles which decreased the total mass of the biocatalyst in the reaction chamber. Therefore, the biocatalytic activity of the damaged chamber decreased and the consequent measurements were no longer reliable.

Reliability assessment of the measurements was based mostly on the following parameters:

1. Chamber difference score (SC)—Over $SC > 4000$ (average), the measurement was declined.
2. Control measurement—Over 5% of error, the measurement was declined.

Each of the experiments carried out by the platform was justified based on the above criterion.

3.5.3. Reproducibility of cyclic reactions

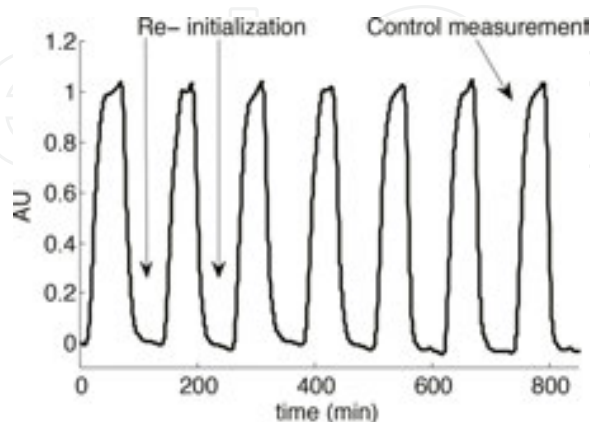


Figure 6. Time plot of the periodic absorbance change during the cyclic measurement (attempt 1, stable layer). The chip is re-initialized between the reaction steps (reaching zero absorbance) by washing out substrate and product completely [22]. The last measurement served as a control.

A crucial feature is the reproducibility of cyclic reactions performed by the system. To check the reproducibility of the test reactions, the MagneChip was filled with MNP biocatalyst, and biotransformation of **L-1a** to **2a** was performed in seven consecutive cycles, while the chip was re-initialized during the steps by washing out the substrate and product completely [22]. The absorbance plot at 290 nm in **Figure 6** with the aid of the previously measured extinction coefficient of the product (**2a**) indicated the concentration changes of **2a**.

The product quantity in cycle by cycle—calculated by taking the integral of the absorbance plot—clearly indicated that the chip was successfully re-initialized in every cycle throughout the experiment, and the reaction was repeated reproducibly seven times (average product quantity of $P = 0.12 \pm 1.5\% \mu\text{mol}$) [22]. The moderate mean value of the chamber difference score $SC = 1322$ (1609 max) reflected negligible changes in the MNP layer.

4. The MagneChip platform: application examples

4.1. Characterization of the PAL reaction with L-phenylalanine (L-1a) in MagneChip

4.1.1. Influence of the substrate flow rate on the biotransformation

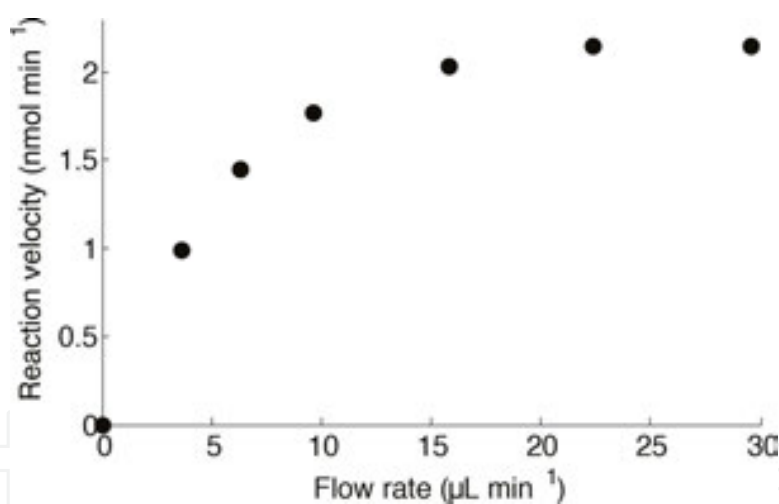


Figure 7. Dependence of the reaction rate of **L-1a** conversion to **2a** on the flow rate in MagneChip filled by *ecMNP*. Saturation was reached at $25 \mu\text{L min}^{-1}$ [22].

MagneChip was filled with *ecMNP* biocatalyst, and biotransformations of **L-1a** to **2a** (**Scheme 1**) at various flow rates were performed in seven consecutive cycles, while the chip was re-initialized at the end of each cycle and a new substrate flow rate was set between 3.6 and $28.6 \mu\text{L min}^{-1}$. The first (reference) measurement was repeated in the last cycle as a control. The negligible difference of specific biocatalytic activity (U_B) between the reference and control measurements (only 3%) and low SC score ($SC < 338$) indicated that the shear forces did not caused irreversible changes on the biocatalytic activity even at high flow rate (up to $28.6 \mu\text{L min}^{-1}$) [22].

The reaction velocity was calculated for each cycles. By increasing the flow rate, the calculated reaction velocity increased until reaching saturation at about $25 \mu\text{L min}^{-1}$ (Figure 7).

4.1.2. Calculation of kinetic parameters

MagneChip was filled with *ec*MNP biocatalyst, and biotransformations of L-1a to 2a (Scheme 1) at various concentrations of L-1a (S_0) were performed in 10 consecutive cycles, while the chip was re-initialized at the end of each cycle and a new substrate concentration was set. It was found that the reaction followed the first-order kinetics up to (S_0) = 3 mM and saturated roughly at (S_0) = 20 mM [22].

The linear fitting method proposed by Lilly et al. [15] was applied for the calculation of the kinetic constants of the biotransformation of L-1a to 2a in the MagneChip (Figure 8, bottom). The values of the kinetic constants are summarized in Table 2 [22].

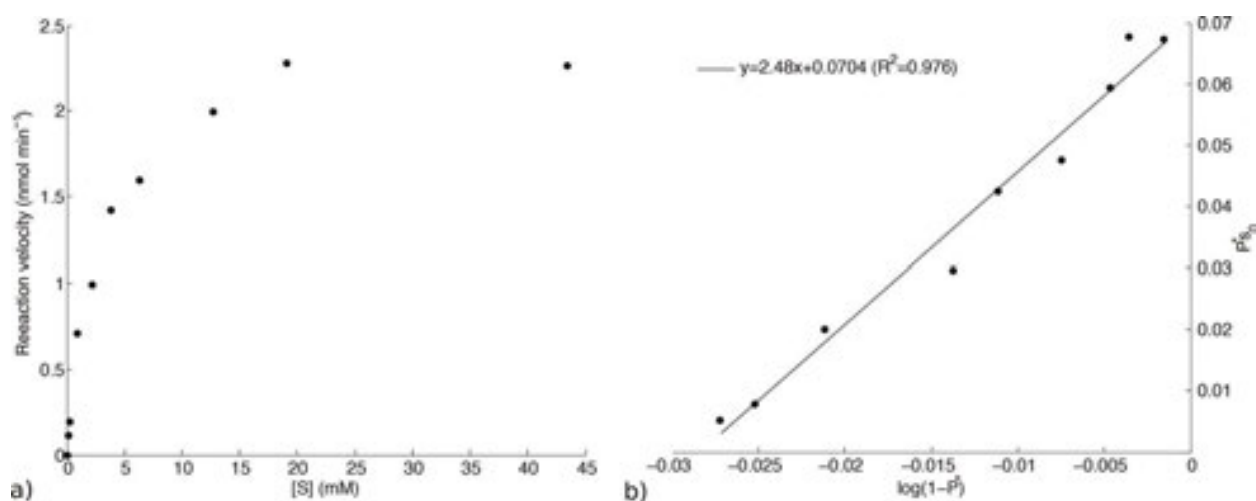


Figure 8. (a) Dependency of the substrate concentration on reaction velocity in MagneChip for the transformation of L-1a to 2a by MNP biocatalyst. Saturation concentration was reached at 20 mM. (b) Linear fit based on the Lilly–Hornby model [15] to determine K_m (resulting in $K_m = 2.5$ mM) [22].

Kinetic parameter	MagneChip	Shake vial
K_m (mM)	2.5	9.1
k_{cat} (s ⁻¹)	2.8×10^{-2}	3.2×10^{-2}
k_{cat}/K_m (s ⁻¹ M ⁻¹)	11.3	3.5

Table 2. Kinetic constants in biotransformation of L-1a to 2a with MNP in shake vial and in MagneChip [22]

It was found that the apparent K_m value was reasonably smaller in MagneChip (2.5 mM) than in shake vial (9.1 mM). Turnover number (k_{cat}) and specificity constant (k_{cat}/K_m) were determined also for both reaction modes. While in the shake vial, the turnover number was somewhat higher ($3.2 \times 10^{-2} \text{ s}^{-1}$) than the in chip ($2.8 \times 10^{-2} \text{ s}^{-1}$), the specificity constant turned

out to be significantly higher in chip ($11.3 \text{ s}^{-1} \text{ M}^{-1}$) as compared with the shake vial ($3.5 \text{ s}^{-1} \text{ M}^{-1}$). This may be attributed to the smaller K_m value in the MagneChip indicating significant contribution of diffusion effects to the higher apparent K_m value in shake vial.

4.2. Effect of particle size on the enzyme activity

The accumulated quantity of *ec*MNPs in the reaction chambers was determined by the embedded resonant magnetometer of the MagneChip device [23]. The measurements revealed that the total mass of the accumulated particles was approximately the same for two different particle sizes ($m = 241.6 \text{ }\mu\text{g}$, *ec*MNP₆₀₀, $d = 600 \text{ nm}$ and $m = 248.3 \text{ }\mu\text{g}$, *ec*MNP₂₅₀, $d = 250 \text{ nm}$) [23]. The total particle mass could be only increased using a binary mixture ($m = 283.6 \text{ }\mu\text{g}$, MNP_{250:600}) of the particles. This experiment resulted in a significantly higher MNP mass (17%) captured in the magnetic chamber as compared with the chamber capacity filled with MNPs of uniform particle sizes [23].

MagneChip was filled with different sized MNP biocatalysts, and biotransformations of L-1a to 2a (Scheme 1) were also performed [23]. Compared with the larger particles (*ec*MNP₆₀₀), the total surface area increased both in the *ec*MNP₂₅₀ (2.5 times) and the mixture cases (2.06 times). Note that differences in biocatalytic activity can be expected only due to changes of transport limitations as the enzyme to MNP mass ratio was kept to be constant of 15% in both cases.

IntechOpen

Figure 9. Specific absorbance of cinnamic acid (2a) at 295 nm at the chip outlet using MNP₆₀₀, MNP₂₅₀, and 1:1 mixture of the two kind of particles in the chip [25].

Results of the measurement using variously sized *ec*MNPs as biocatalysts are summarized in **Figure 9**. In fact, the *ec*MNP₆₀₀-filled chambers yielded the lowest final concentration of product as indicated by the lowest specific absorbance ($\text{AU} = 1.07$, at 295 nm) at the chip outlet. Filling the chip by *ec*MNP₂₅₀ resulted in an increase of the measured absorbance by 46% ($\text{AU} = 1.56$, at 295 nm). Because the chambers contained the same filling mass ($m = 241.6 \text{ }\mu\text{g}$ for *ec*MNP₆₀₀

and $m = 248.3 \mu\text{g}$ for $ec\text{MNP}_{250}$) and therefore the same enzyme amount, the difference between the MNP_{250} - and the MNP_{600} -filled reactors can only be attributed to other factors, for example, to the differences in total surface area [23].

The major difference can also stem from the remarkably smaller average microchannel diameters between the particles within the $ec\text{MNP}_{250}$ -filled chamber as compared to the $ec\text{MNP}_{600}$ -filled one. This can result in shortened diffusion path and therefore better mass transport [23]. An additional 40% increment was achieved using the 1:1 particle mixture, which was obviously resulted as a synergy of the higher enzyme content (17%) due to the higher chamber capacity and enhanced transport phenomena due to the small average microchannel diameter [25].

4.3. Testing multiple substrates in MagneChip

Substrate screening experiments were performed with a single $ec\text{MNP}$ -loading in the chip passing the solutions of the different substrates (**Scheme 1: L-1a** and **rac-1b-f**) through the same chip according to a predefined sequence [22]. The intensive washing procedure between the individual tests with various substrates ensured complete removal of any substrate or product from the preceding cycle (reaction). In the first cycle, the ammonia elimination was measured from **L-1a** (the natural substrate of PAL). This reaction was chosen as reference for comparison to the other elimination reactions of PAL from the further substrates (**rac-1b-f**). The difference between the initial and final (control) measurement with **L-1a** was found to be only 1.5%, while the SC score remained below 2000. Surprisingly, in the MagneChip device, higher biocatalytic activities (U_B) were observed with four of the unnatural substrates (**rac-1b,c,e,f**), than with the natural substrate L-phenylalanine **L-1a** (**Figure 10**).

IntechOpen

Figure 10. Comparison of the specific biocatalytic activity of $Pc\text{PAL}$ immobilized on MNPs with substrates **L-1a** and **rac-1b-f** in MagneChip system $[(S) = 20 \text{ mM}, \text{flow rate: } 48.6 \mu\text{L min}^{-1}]$ [22]. *Control measurement.

Noteworthy, all the four unnatural substrates (*rac*-**1b,c,e,f**) which were transformed by the MNP biocatalyst with higher specific biocatalytic activity (U_B) than that of L-phenylalanine **L-1a** contained slightly more electron-withdrawing aromatic moieties than the phenyl group. This difference from the productivity ranks observed with homogenous *PcPAL* so far may be due to the reduced contribution of the reverse reaction (equilibrium effect) to the apparent forward reaction rates in the continuous-flow system at high flow rates [22].

4.4. Characterization of an enzyme reaction with a novel substrate

By a reaction performed in the MagneChip device, it was first demonstrated that PAL can catalyze the ammonia elimination from the acyclic DL-propargylglycine (PG) to yield (*E*)-pent-2-ene-4-ynoate, indicating new opportunities to extend the MIO-enzyme toolbox toward acyclic substrates. Deamination of PG, being acyclic, cannot involve a Friedel–Crafts-type attack at an aromatic ring [18].

MagneChip, filled by PAL-*ec*MNPs, was used for the microscale biotransformation of DL-propargylglycine in sodium carbonate-buffered D₂O. The device enabled to detect the formation of (*E*)-pent-2-en-4-ynoate at 242 nm and to produce measurable quantities of the product for recording ¹H-NMR spectra without any work-up. Besides the significant increase of the UV-signal at 242 nm (up to $A = 1.2$) in the in-line UV-cell (**Figure 11**), the appearance of olefin hydrogen signals in the ¹H-NMR spectrum of the reaction mixture [at $\delta = 6.34$ (*d*) and 6.85 (*d*) ppm] indicated unambiguously the formation of (*E*)-pent-2-en-4-ynoate. On the other hand, emergence of the UV signal at 274 nm during the process indicated the formation of further by-product(s) apart from (*E*)-pent-2-en-4-ynoate (**Figure 11**).

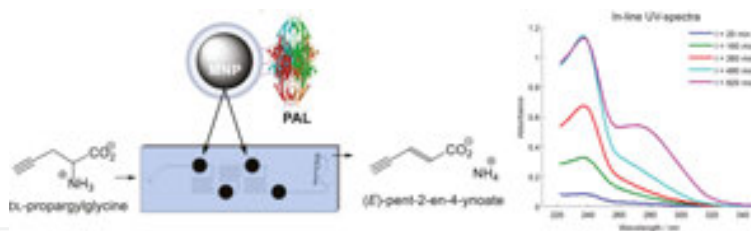


Figure 11. Ammonia elimination from DL-propargylglycine in MagneChip filled with PAL immobilized on MNPs and equipped with in-line UV-Vis detector (reaction in D₂O at pD 8.8, 37°C) [18]. The progress of the reaction was followed by full UV-spectra.

5. Conclusion

Our results proved that the MagneChip microfluidic device is a reliable, reproducible, and efficient tool which was capable of fast, reliable, and fully automated screening and kinetic characterization of *PcPAL* substrates using minimal solvent (~500 μ l) and biocatalyst (~1 mg MNP) amounts for a test compound. Compared with shake vial, the volumetric productivity of the MNP biocatalyst in the chip exceeded the one of the shake vial by more than three orders

of magnitude. The platform was also capable of studying enzymatic reactions with undiscovered substrates of *PcPAL*. The above results suggest that the MagneChip platform would be successfully utilized as a novel and flexible tool for enzyme-catalyzed biotransformations.

Author details

Ferenc Ender^{1*}, Diána Weiser² and László Poppe^{2,3}

*Address all correspondence to: ender@eet.bme.hu

1 Department of Electron Devices, Budapest University of Technology and Economics, Budapest, Hungary

2 Department of Organic Chemistry and Technology, Budapest University of Technology and Economics, Budapest, Hungary

3 SynBiocat LLC, Lázár deák, Budapest, Hungary

References

- [1] Ehrfeld W, Hessel V, and Haverkamp V, "Microreactors," *Ullmann's Encycl Ind Chem*, pp. 173–198, 2012.
- [2] Weiler A, Junkers M. Using microreactors in chemical synthesis: batch process versus continuous flow. *Pharm Technol*. 2009;S6:S10–S11.
- [3] Besanger TR, Chen Y, Deisingh AK, Hodgson R, Jin W, Mayer S, et al. Screening of inhibitors using enzymes entrapped in sol-gel-derived materials. *Anal Chem*. 2003;75:2382–91. doi:10.1021/ac026370i CCC
- [4] Urban PL, Goodall DM, Bruce NC. Enzymatic microreactors in chemical analysis and kinetic studies. *Biotechnol Adv*. 2006;24:42–57. doi:10.1016/j.biotechadv.2005.06.001
- [5] Webb D, Jamison TF. Continuous flow multi-step organic synthesis. *Chem Sci*. 2010;1:675. doi:10.1039/C0SC00381F
- [6] Nisha S, Karthick SA, Gobi N. A review on methods, application and properties of immobilized enzyme. *Chem Sci Rev Lett*. 2012;1:148–55.
- [7] Mu X, Qiao J, Qi L, Dong P, Ma H. Poly(2-vinyl-4,4-dimethylazlactone)-functionalized magnetic nanoparticles as carriers for enzyme immobilization and its application. *ACS Appl Mater Interfaces*. 2014;6:21346–54. doi:10.1021/am5063025

- [8] He P, Greenway G, Haswell SJ. Development of enzyme immobilized monolith micro-reactors integrated with microfluidic electrochemical cell for the evaluation of enzyme kinetics. *Microfluid Nanofluid.* 2010;8:565–73. doi:10.1007/s10404-009-0476-8
- [9] Seong GH, Heo J, Crooks RM. Measurement of enzyme kinetics using a continuous-flow microfluidic system. *Anal Chem.* 2003;75:3161–7. doi:10.1021/ac034155b
- [10] Lien K-Y, Lee W-C, Lei H-Y, Lee G-B. Integrated reverse transcription polymerase chain reaction systems for virus detection. *Biosens Bioelectron.* 2007;22:1739–48. doi:10.1016/j.bios.2006.08.010
- [11] Liu Y, Yang D, Yu T, Jiang X. Incorporation of electrospun nanofibrous PVDF membranes into a microfluidic chip assembled by PDMS and scotch tape for immunoassays. *Electrophoresis* 2009;30:3269–75. doi:10.1002/elps.200900128
- [12] Do J, Ahn CH. A polymer lab-on-a-chip for magnetic immunoassay with on-chip sampling and detection capabilities. *Lab Chip.* 2008;8:542–9. doi:10.1039/B715569G
- [13] Li Y, Xu X, Yan B, Deng C, Yu W, Yang P, et al. Microchip reactor packed with metal-ion chelated magnetic silica microspheres for highly efficient proteolysis. *J Proteome Res.* 2007;6:2367–75. doi:10.1021/pr060558r
- [14] Kerby MB, Legge RS, Tripathi A. Measurements of kinetic parameters in a microfluidic reactor. *Anal Chem.* 2006;78:8273–80. doi:10.1021/ac061189l
- [15] Lilly MD, Hornby WE, Crook EM. The kinetics of carboxymethylcellulose-ficin in packed beds. *Biochem J.* 1966;100:718–23. doi:10.1042/bj1000718
- [16] Slovakova M, Minc N, Bilkova Z, Smadja C, Faigle W, Fütterer C, et al. Use of self-assembled magnetic beads for on-chip protein digestion. *Lab Chip.* 2005;5:935–42. doi:10.1039/B504861C
- [17] Netto C, Toma H, Andrade L. Superparamagnetic nanoparticles as versatile carriers and supporting materials for enzymes. *J Mol Catal B Enzym.* 2013;85–86:71–92. doi:10.1016/j.molcatb.2012.08.010
- [18] Weiser D, Bencze LC, Bánóczy G, Ender F, Kiss R, Kókai E, et al. Phenylalanine ammonia-lyase-catalyzed deamination of an acyclic amino acid: enzyme mechanistic studies aided by a novel microreactor filled with magnetic nanoparticles. *Chem BioChem.* 2015;16:2283–88. doi:10.1002/cbic.201500444
- [19] Xu J, Yang H, Fu W, Du K, Sui Y, Chen J, et al. Preparation and magnetic properties of magnetite nanoparticles by sol-gel method. *J Magn Magn Mater.* 2007;309:307–11. doi:10.1016/j.jmmm.2006.07.037
- [20] Faraji M, Yamini Y, Rezaee M. Magnetic nanoparticles: synthesis, stabilization, functionalization, characterization, and applications. *J Iran Chem Soc.* 2010;7:1–37. doi:10.1007/BF03245856

- [21] Akbarzadeh A, Samiei M, Davaran S. Magnetic nanoparticles: preparation, physical properties and applications in biomedicine. *Nanoscale Res Lett.* 2012;7:144. doi: 10.1186/1556-276X-7-144
- [22] Bradford MM. A rapid and sensitive method for the quantitation of microgram quantities of protein utilizing the principle of protein-dye binding. *Anal Biochem.* 1976;72:248–54. doi:10.1016/0003-2697(76)90527-3
- [23] Ender F, Weiser D, Nagy B, Bencze LC, Paizs C, Pálovics P, et al. “Microfluidic multiple cell chip reactor filled with enzyme-coated magnetic nanoparticles – An efficient and flexible novel tool for enzyme catalyzed biotransformations,” *J Flow Chem*, vol. 6, no. 1, pp. 43–52, 2016.
- [24] Pamme N. On-chip bioanalysis with magnetic particles. *Curr Opin Chem Biol.* 2012;16:436–43. doi:10.1016/j.cbpa.2012.05.181
- [25] Ender F, Weiser D, Vitéz A, Sallai G, Németh M, Poppe L. In-situ measurement of magnetic nanoparticle quantity in a microfluidic device. *Microsyst Technol.* 2015;21:1–12. doi:10.1007/s00542-015-2749-3